

Stability charts for granular embankments on soft soils with linearly increasing undrained strength

Guo H. Lei¹, H.M. Zhang¹, F.X. Liu¹, and F. Zhang¹

¹ Key Laboratory of Geomechanics and Embankment Engineering of the Ministry of Education, Geotechnical Research Institute, Hohai University, 1, Xikang Road, Nanjing 210098, China.

ABSTRACT

This paper presents an upper bound limit analysis of the stability of granular embankments on soft soils with linearly increasing undrained strength. Based on a deep-seated, kinematically admissible, rotational failure mechanism, an analytical solution is derived for calculating the factor of safety, which is defined as the ratio of the shear strength to the mobilized strength of the embankment and foundation soil. A set of stability charts is presented in a wide range of parameters. The analytical solution is well organized such that the stability charts require no iteration to evaluate the safety factor. These charts provide a convenient tool for assessing the safety of granular embankments on soft soils in practical applications such as sea dykes and breakwaters.

Keywords: limit analysis; stability chart; embankment; slope; soft soil; linearly increasing undrained strength

1 INTRODUCTION

Since the pioneering work of Taylor (1937), many stability charts have been proposed based on various assumptions and considerations. Among them, only a limited number of charts can be utilized to preliminarily assess the stability of embankments on soft soils. Leshchinsky (1987) and Leshchinsky and Smith (1989) presented two sample stability charts for granular embankments (without cohesion) over soft soils with uniform and linearly-increasing undrained strength with depth, respectively. These charts were derived using the variational limit-equilibrium method suggested by Baker and Garber (1978). Evaluating a safety factor for an embankment using the charts has to be done iteratively. Low (1989) developed a set of stability charts for embankments on soft soils with uniform undrained strength. These charts were derived based on an approximate semi-analytical approach to the limit equilibrium method. The factor of safety of embankment was defined as the ratio of the overturning moment to the resisting moment, and the shear strength of embankment material was characterized by both cohesion and internal friction. Recently, by using the finite-element upper and lower bound limit analysis methods, Qian et al. (2015) and Lim et al. (2016) developed stability charts for purely cohesive and purely frictional embankment materials placed on purely cohesive soil with uniform undrained strength, respectively. It is evident that the abovementioned stability charts, except the two sample charts with the necessity for iterations derived by Leshchinsky and Smith (1989), are only applicable to embankments on soft soils with uniform undrained shear strength. However, it is well recognized that in practical

situations, undrained shear strength of soil almost always increases with depth. This has already been considered in some undrained stability analyses of slopes in normally consolidated soils whose strengths are finite at the crest and vary linearly with depth (Gibson and Morgenstern 1962; Hunter and Schuster 1968; Booker and Davis 1972; Chen et al. 1975; Chen and Sawada 1983; Koppula 1984; Shen and Brand 1985; Yu et al. 1998; Griffiths and Yu 2015). There is still a lack of convenient stability charts for granular embankments founded on soft soils with linearly increasing undrained strength. For this reason, this paper presents a rigorous upper bound limit analysis of the embankment stability. An analytical solution is derived for calculating the factor of safety, which is defined as usual as the ratio of the shear strength to the mobilized shear strength of soil. Stability charts are constructed without the necessity for iterations to evaluate the safety factors.

2 PROBLEM DESCRIPTION

Figure 1 shows schematically a model of limit analysis of the stability of a granular embankment on a soft soil. The groundwater table is assumed to be located at the ground surface. In Fig. 1, H and β represent the height and inclination of the embankment slope, respectively; γ and ϕ are the unit weight and the internal friction angle of embankment fill; and the undrained strength of the soft soil is assumed to be

$$s_u = s_{u0} + \rho z \quad (1)$$

where z is the depth from the top surface of the soft soil; s_{u0} is the undrained strength at the top of the soft soil;

and ρ is the rate of increase in the undrained strength of the soft soil with depth.

As usual, the factor of safety of the embankment is defined as

$$F_s = \frac{s_u}{s_{um}} = \frac{\tan \varphi}{\tan \varphi_m} \quad (2)$$

where s_{um} and ϕ_{m} are the mobilized undrained strength of the soft soil and the mobilized internal friction angle of the embankment fill, respectively.

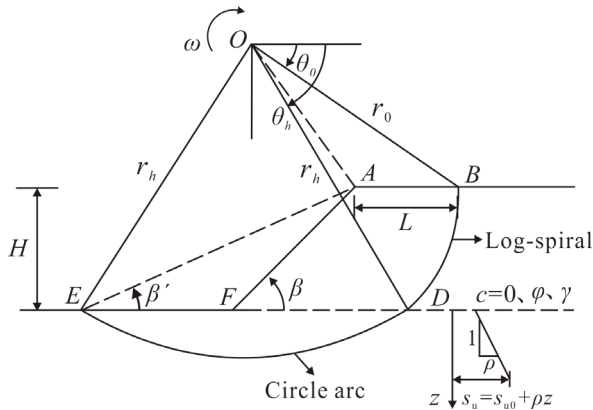


Fig. 1. A model of limit analysis of stability of granular embankment on soft soil with increasing undrained strength.

3 UPPER BOUND LIMIT ANALYSIS

According to the upper bound theorem of plasticity limit analysis (Chen 1975), the failure surface in fulfillment of non-associated flow rule and kinematical admissibility is a combination of a log-spiral in the embankment and a circle arc in the foundation soil, as shown in Fig. 1. The log-spiral and the circle arc can be described as follows.

$$r = r_0 e^{(\theta - \theta_0) \frac{\tan \varphi}{F_s}} \quad (3)$$

$$r = r_h = r_0 \mathbf{e}^{(\theta_h - \theta_0) \frac{\tan \varphi}{F_s}} \quad (4)$$

where r and θ are the radial coordinate and the angular coordinate measured clockwise from the horizontal in the polar coordinate system shown in Fig. 1; r_0 and θ_0 are the polar coordinates of the intersectional point B of the slip surface and the crest of the embankment; and θ_h is the polar angle of the intersectional point D of the slip surface and the top of the soft soil.

Based on the above failure mechanism, an upper bound on the factor of safety of the embankment can be determined by equating the rate of work W done by soil weight to the rate of internal energy dissipation D . Following the same procedures for obtaining the expressions of W and D for a homogeneous slope as presented by Chen (1975), the expressions of W and D for the embankment on soft soil are derived as follows.

$$W = \gamma \omega r_0^3 (f_1 + f_2 - f_3 - f_4 - f_5) \quad (5)$$

$$D = \frac{S_{u0}}{\tan \varphi} \omega r_0^2 d \quad (6)$$

where ω is the angular speed of rotation of the sliding mass ABDEF as shown in Fig. 1; f_1, f_2, f_3, f_4 and f_5 are the coefficients of the rate of work done by soil weight of the sliding masses OBDO, ODEO, OBAO, OAEO and AFEA, respectively, as shown in Fig. 1; and

$$f_1 = \frac{1}{3} \left[1 + 9 \left(\frac{\tan \varphi}{F_s} \right)^2 \right]^{-1} \left[-3 \frac{\tan \varphi}{F_s} \cos \theta_0 - \sin \theta_0 \right] \quad (7)$$

$$+ \left(3 \frac{\tan \varphi}{F_s} \cos \theta_h + \sin \theta_h \right) e^{3(\theta_h - \theta_0) \frac{\tan \varphi}{F_s}} \quad (8)$$

$$f_3 = \frac{1}{6} \sin \theta_0 \frac{L}{r_0} \left(2 \cos \theta_0 - \frac{L}{r_0} \right) \quad (9)$$

$$f_4 = \frac{1}{6} e^{(\theta_h - \theta_0) \frac{\tan \varphi}{F_s}} \frac{H}{r_0} \frac{\sin(\theta_h - \beta')}{\sin \beta'} \times \left[\cos \theta_0 - \frac{L}{r_0} - e^{(\theta_h - \theta_0) \frac{\tan \varphi}{F_s}} \cos \theta_h \right] \quad (10)$$

$$f_5 = \frac{1}{6} \left(\frac{H}{r_0} \right)^2 (\cot \beta' - \cot \beta) \left[2 \cos \theta_0 - 2 \frac{L}{r_0} - \frac{H}{r_0} \cot \beta - e^{(\theta_h - \theta_0) \frac{\tan \varphi}{F_s}} \cos \theta_h \right] \quad (11)$$

$$\frac{H}{r_0} = e^{(\theta_h - \theta_0) \frac{\tan \varphi}{F_s}} \sin \theta_h - \sin \theta_0 \quad (12)$$

$$\begin{aligned} \frac{L}{r_0} = & \cos \theta_0 + e^{\frac{(\theta_h - \theta_0) \tan \varphi}{F_s}} \cos \theta_h \\ & - \left[e^{\frac{(\theta_h - \theta_0) \tan \varphi}{F_s}} \sin \theta_h - \sin \theta_0 \right] \cot \beta' \end{aligned} \quad (13)$$

$$d = 2 \frac{\tan \varphi}{F_s} e^{2(\theta_h - \theta_0) \frac{\tan \varphi}{F_s}} \left\{ \left(\frac{\pi}{2} - \theta_h \right) - \frac{\rho H}{s_{u0}} \left(\frac{H}{r_0} \right)^{-1} \right. \\ \left. \times e^{(\theta_h - \theta_0) \frac{\tan \varphi}{F_s}} \left[\left(\frac{\pi}{2} - \theta_h \right) \sin \theta_h - \cos \theta_h \right] \right\} \quad (14)$$

The following equation can be obtained by equating Eqs. (5) and (6).

$$\frac{S_{u0}}{\gamma H \tan \varphi} = \frac{1}{g(\theta_0, \theta_b, \beta')} \quad (15)$$

where β' is the angle included between the line AE and the horizontal as shown in Fig. 1; and

$$g(\theta_0, \theta_h, \beta') = \left(\frac{H}{r_0} \right) \frac{d}{f_1 + f_2 - f_3 - f_4 - f_5} \quad (16)$$

Therefore, the least upper bound to the factor of safety of the embankment is determined from

$$\frac{s_{u0}}{\gamma H \tan \varphi} = \frac{1}{\min[g(\theta_0, \theta_h, \beta')]} \quad (17)$$

It can be observed from Eqs. (7) to (15) that the only input parameters required for the calculation are β , $\rho H/s_{u0}$ and $\tan \varphi/F_s$. For a given set of values of θ_0 , θ_h and β' , the result of $g(\theta_0, \theta_h, \beta')$ can be determined from Eq. (16). Its minimum value corresponding to the least upper bound to the factor of safety of the embankment can be search for using an optimization procedure as described in the next section. Substituting it into Eq. (17) yields the critical value of the dimensionless quantity of $s_{u0}/(\gamma H \tan \varphi)$. Therefore, for an embankment with given values of β and $\rho H/s_{u0}$, there is a unique relationship between $\tan \varphi/F_s$ and $s_{u0}/(\gamma H \tan \varphi)$, which is called the stability number of the embankment (Michalowski 2002).

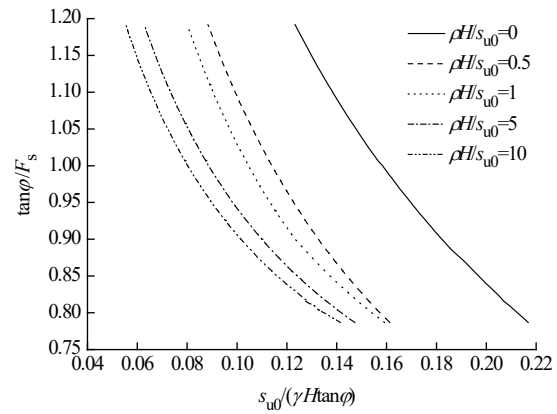
4 SOLVING PROCEDURE

An optimization method proposed by Chen (1992) is adopted to find the least upper bound to the factor of safety in order to avoid missing the global minimum. The method uses random search to find the global minimum and performs the minimization procedure until the band widths of search variables become less than predefined values. It has been proven to be efficient in finding the least upper bounds to the critical height of slopes in the previous works by Gao et al. (2013). For details of the method, see the source reference.

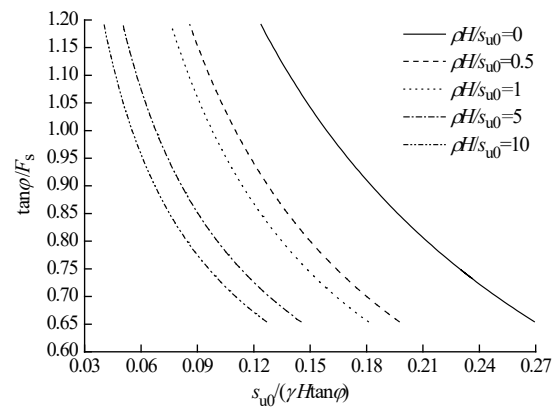
For a slope of given values of β , $\rho H/s_{u0}$ and $\tan \varphi/F_s$, independent variables in the minimization process include angles θ_0 , θ_h and β' (see Fig. 1). In the search for the minimum value of $g(\theta_0, \theta_h, \beta')$, the minimization procedure is performed until the band widths become less than 0.001° for angles θ_0 , θ_h and β' .

5 STABILITY CHARTS

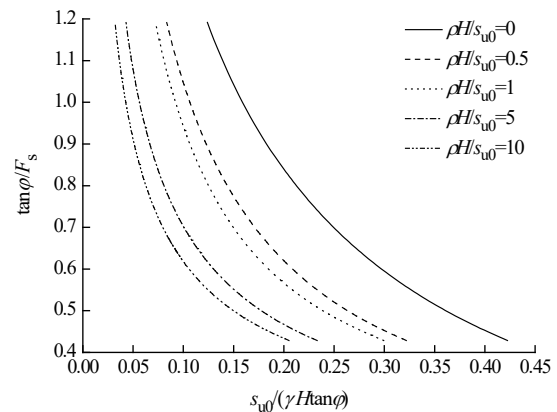
Figure 2 shows the relationship between the critical values of $s_{u0}/(\gamma H \tan \varphi)$ and $\tan \varphi/F_s$ for various values of β and $\rho H/s_{u0}$. Typical values of s_{u0} and ρ for most soft clays presented by Koppula (1984) are adopted to determine the parameter $\rho H/s_{u0}$ for calculation. It can be seen from Fig. 2 that the values of $\tan \varphi/F_s$ decrease with the increases in the stability number $s_{u0}/(\gamma H \tan \varphi)$ and the value of $\rho H/s_{u0}$. This reflects that for an embankment with a given value of φ , the safety of the embankment increases with the strength of the soft soil.



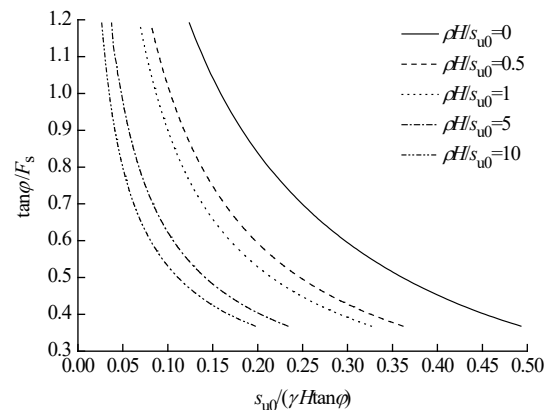
(a) $\beta = 45^\circ$ (slope ratio of 1.0H:1V)



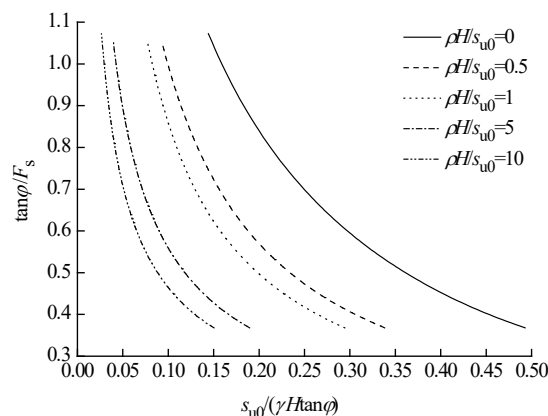
(b) $\beta = 33.69^\circ$ (slope ratio of 1.5H:1V)



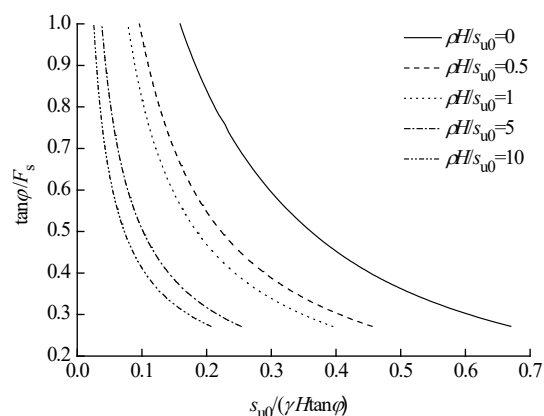
(c) $\beta = 26.57^\circ$ (slope ratio of 2.0H:1V)



(d) $\beta = 21.8^\circ$ (slope ratio of 2.5H:1V)



(e) $\beta = 18.43^\circ$ (slope ratio of 3.0H:1V)



(f) $\beta = 15.95^\circ$ (slope ratio of 3.5H:1V)

Fig. 2. Stability charts for granular embankments on soft soils with linearly increasing undrained strength.

6 CONCLUSION

Based on a kinematically admissible rotational failure mechanism, a rigorous analytical approach is derived for the upper-bound limit analysis of the stability of granular embankments on soft soils with linearly increasing undrained strength with depth. Stability charts are presented, allowing for straightforward calculation of the factors of safety of embankments without the necessity for iterations. These charts provide an efficient tool for the preliminary assessment of the safety of granular embankments on soft soils with linearly increasing undrained strength with depth as encountered in most practical situations.

ACKNOWLEDGEMENTS

This study was sponsored by the National Natural Science Foundation of China (51578213, 51508160) and the Fundamental Research Funds for the Central Universities of China (2017B00814, 2017B20614).

REFERENCES

- Baker, R. and Garber, M. (1978). Theoretical analysis of the stability of slopes. *Géotechnique*, 28(4), 395-411.
- Booker, J. R. and Davis, E. H. (1972). A note on a plasticity solution to the stability of slopes in inhomogeneous clays. *Géotechnique*, 22(3), 509-513.
- Chen, W. F. (1975). *Limit analysis and soil plasticity*, Elsevier, Amsterdam, the Netherlands.
- Chen, W. F. and Sawada, T. (1983). Earthquake-induced slope failure in nonhomogeneous, anisotropic soils. *Soils and Foundations*, 23(2), 125-139.
- Chen, W. F., Snitbhan, N., and Fang, H. Y. (1975). Stability of slopes in anisotropic, nonhomogeneous soils. *Canadian Geotechnical Journal*, 12(1), 146-152.
- Chen, Z. Y. (1992). Random trials used in determining global minimum factors of safety of slopes. *Canadian Geotechnical Journal*, 29(2), 225-233.
- Gao, Y. F., Zhang, F., Lei, G. H., and Li, D. Y. (2013). An extended limit analysis of three-dimensional slope stability. *Géotechnique*, 63(6), 518-524.
- Gibson, R. E. and Morgenstern, N. (1962). A note on the stability of cuttings in normally consolidated clay. *Géotechnique*, 12(3), 212-216.
- Griffiths, D. V. and Yu, X. (2015). Another look at the stability of slopes with linearly increasing undrained strength. *Géotechnique*, 65(10), 824-830.
- Hunter, J. H. and Schuster, R. L. (1968). Stability of simple cuttings in normally consolidated clay. *Géotechnique*, 18(3), 372-378.
- Koppula, S. D. (1984). On stability of slopes in clays with linearly increasing strength. *Canadian Geotechnical Journal*, 21(3), 577-581.
- Leshchinsky, D. (1987). Short-term stability of reinforced embankment over clayey foundation. *Soils and Foundations*, 27(3), 43-57.
- Leshchinsky, D. and Smith, D. S. (1989). Deep-seated failure of a granular embankment over clay: Stability analysis. *Soils and Foundations*, 29(3), 105-114.
- Lim, K., Lyamin, A. V., Cassidy, M. J., and Li, A. J. (2016). Three-dimensional slope stability charts for frictional fill materials placed on purely cohesive clay. *International Journal of Geomechanics*, 16(2), 04015042.
- Low, B. K. (1989). Stability analysis of embankments on soft ground. *Journal of Geotechnical Engineering*, 115(2), 211-227.
- Michalowski, R. L. (2002). Stability charts for uniform slopes. *Journal of Geotechnical and Geoenvironmental Engineering*, 128(4), 351-355.
- Qian, Z. G., Li, A. J., Merifield, R. S., and Lyamin, A. V. (2015). Slope stability charts for two-layered purely cohesive soils based on finite-element limit analysis methods. *International Journal of Geomechanics*, 15(3), 06014022.
- Shen, J. M. and Brand, E. W. (1985). Discussion of 'On stability of slopes in clays with linearly increasing strength' by Koppula, S. D. *Canadian Geotechnical Journal*, 22(3), 419-421.
- Taylor, D. W. (1937). Stability of earth slopes. *Journal of the Boston Society of Civil Engineers*, 24(3), 197-246.
- Yu, H. S., Salgado, R., Sloan, S. W., and Kim, J. M. (1998). Limit analysis versus limit equilibrium for slope stability. *Journal of Geotechnical and Geoenvironmental Engineering*, 124(1), 1-11.